Heat Capacity of Pd-Si, Ni-Si-B and Zr-Based Metallic Glasses

Heat Capacity of Pd-Si, Ni-Si-B and Zr-Based Metallic Glasses *

Takeshi KANOMATA[a], Yuka SATO[a], Yasuhiro SUGAWARA[a], Shigeyuki ABURATANI[a],

Hisamichi KIMURA[b], Takejiro KANEKO[b], Akihisa INOUE[b] and Tsuyoshi MASUMOTO[b]

[a]*Department of Applied Physics, Faculty of Engineering, Tohoku Gakuin University, Tagajo, 985 Miyagi, Japan*
[b]*Institute for Materials Research, Tohoku University, Sendai, 980-77 Japan*
(Received January 15, 1997)

The specific heat of metallic glasses containing Si and B ($Ni_{78}Si_{10}B_{12}$ and $Pd_{80}Si_{20}$) and Zr-based metallic glasses($Zr_{60}Al_{15}Cu_{15}Ni_{7.5}Co_{2.5}$, $Zr_{65}Al_{17.5}Cu_{7.5}$ and $Zr_{67}Cu_{33}$) was measured in the temperature range 77-800 K using an a.c. calorimeter. Several exothermic and endothermic processes were observed correspondingly to the transformation sequences for complete crystallization of all the glasses. The structural relaxation process appears with a decrease in heat capacity. For Ni-Si-B and Pd-Si glasses an abrupt increase in the specific heat is observed at the glass transition temperature T_g. For Zr-based glasses, however, a monotonous increase in the specific heat is observed just below T_g. Then the specific heat makes a peak and decrease abruptly with increasing temperature. The height of the peak increases with heating rate.

KEYWORDS: metallic glass, specific heat, glass transition, Zr-based metallic glass

1. Introduction

It is important to investigate thermal properties in order to understand the mechanism of various kinds of phase transitions in amorphous alloys and metallic glasses. There have been a number of investigations of the structural relaxation, the glass transition and the crystallization sequences of various amorphous alloys. The thermal properties of these phenomena were mainly studied using a differential thermal analysis method or a differential scanning calorimeter with high heating rate. Using these methods is meaningful since the structural relaxation and crystallization sequence of amorphous alloys are a rate process. It is also considered to be important to examine the thermal properties using a conventional calorimeter with low heating rate to investigate the thermodynamics of the phase transition.

Metallic glasses are generally produced from the highly undercooled liquid state by rapid cooling at a critical cooling velocity v_c lager than 10^4 $K \cdot s^{-1}$. Among them the M-Si-B (M = 3d or 4d transition metals) metallic glasses are reported to be prepared with relatively slow cooling rate. Masumoto et al. have investigate their crystallization processes by transmission electron microscopy of alloys heated on the hot stage of a microscope and a scanning thermal analysis and then by measuring the temperature variation of electric resistance and micro-hardness[1-5].

Recently, Inoue et al. have found that a bulk metallic glass can be prepared even by conventional casting techniques at relatively slow cooling rates. They have found that a number of metallic glasses can be formed by quenching at v_c smaller than 10^2 $K \cdot s^{-1}$ for Zr-Cu alloy system[6]. They have also revealed that the addition of the elements Al, Ni and Co to binary Zr-Cu alloys increases extremely the supercooled liquid region. Multinary Zr-Cu based metallic glasses have the wide supercooled liquid region exceeding 100 K. The supercooled region is defined by the temperature range, $\Delta T_x = T_x - T_g$, between the glass transition temperature(T_g) and the crystallization temperature(T_x). Kimura et al. have studied the metallurgical and physical properties in the glass state below T_g and in the supercooled liquid state in the temperature range ΔT_x for Zu-Cu based metallic glasses[7]. The results show that multinary $Zr_{60}Al_{15}Cu_{15}Ni_{7.5}Co_{2.5}$ alloy is extremely softened in the temperature range of the supercooled liquid region and the thermal expansion coefficient of this alloy is very small of $0.9 \times 10^{-5} K^{-1}$, at temperatures below T_g. Furthermore, they have reported that the temperature coefficient of Young's modulus is of the order as small as $\sim 10^{-5}$ K^{-1} for this alloy.

Little is known about specific heat C_p in the glass state below T_g and in the supercooled liquid state in the temperature range ΔT_x for Zr-Cu based metallic glasses. In this paper, we have studied the temperature variation of the specific heat of $Pd_{80}Si_{20}$ and $Ni_{78}Si_{10}B_{12}$ metallic glasses containing metalloid elements to obtain new insight for the thermal properties of the supercooled liquid state and the glass transition itself. We report also the

results of the temperature variation of the specific heat at temperatures around T_g of $Zr_{67}Cu_{33}$, $Zr_{65}Al_{17.5}Cu_{27.5}$ and $Zr_{60}Al_{15}Cu_{15}Ni_{7.5}Co_{2.5}$ metallic glasses. Differential thermal analysis was also carried out to examine the crystallization process. Some parts of experimental results here were reported in ref.(8) and (9).

2. Experimental procedures

Alloys used for the metallic glasses were prepared by arc melting a mixture of constituent elements with desired compositions in a purified argon gas atmosphere. The specimens were prepared by a single roller melt-spinning technique in an argon gas atmosphere in the form of about $40 \sim 100$ μ m thick ribbon. The specific heat was measured using an a.c. calorimeter (Type ACC-VL1 for low temperature and Type ACC-1 for high temperature, SINKU-RIKO Co.). The heating rate was 1 K·min⁻¹ for the specific measurements of $Ni_{78}Si_{10}B_{12}$ and $Pd_{80}Si_{20}$ alloys and 5 K·min⁻¹ for $Zr_{65}Al_{7.5}Cu_{27.5}$ alloy. For the specific heat measurements of $Zr_{67}Cu_{33}$ and $Zr_{60}Al_{15}Cu_{15}Ni_{7.5}Co_{2.5}$, the heating rate was changed variously. There is some error in the absolute value of specific heat since it is not easy to determine exactly the thickness of amorphous thin film owing to scattering of the thickness values over the film. The endothermic and exothermic reactions associated with T_g and T_x and the crystallization process was also examined by differential scanning calorimetry(DSC).
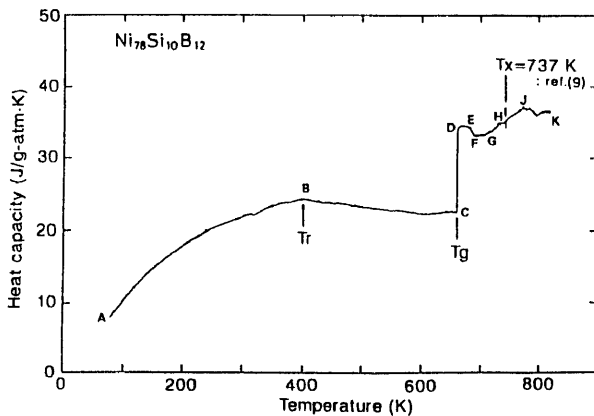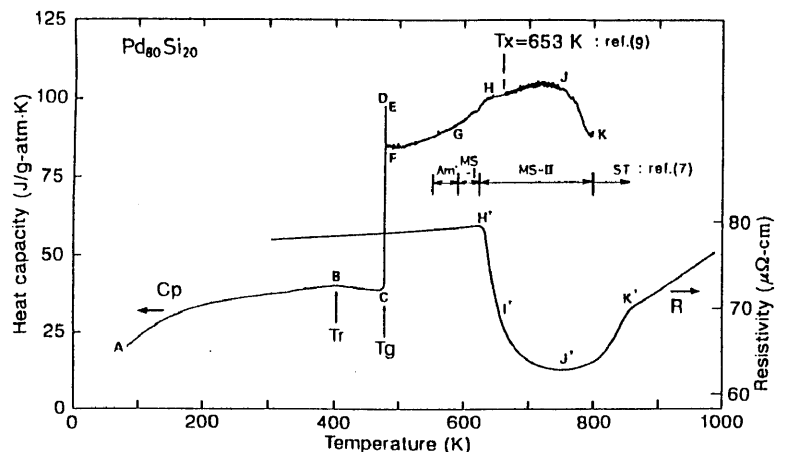

Fig. 1. Temperature dependence of the specific heat of $Ni_{78}Si_{10}B_{12}$ metallic glass[8]. T_x is the crystallization temperature[3].

Fig. 2. Temperature dependence of the specific heat of $Pd_{80}Si_{20}$ metallic glass[8]. T_x is the crystallization temperature[3].

3. Experimental results and discussions

3.1 $Ni_{78}Si_{10}B_{12}$ and $Pd_{80}Si_{20}$

Figures 1 and 2 show the heat capacity vs. temperature cures for $Ni_{78}Si_{10}B_{12}$ and $Pd_{80}Si_{20}$ metallic glasses. As seen in the figures, the temperature dependence of the specific heat can be characterized for both amorphous alloys as follows. (1) The specific heat increases at first with increasing temperature (A-B). (2) It decreases after reaching a broad maximum around B(T_r)(B-C). (3) It increases discontinuously at C(T_g) (C-D). (4) It decreases sharply at E (E-F). (5) It increases at temperature from F to G and sharply from G to H. (6) After showing a shoulder around H-I, it increases again to J. (7) Finally it decreases after reaching a maximum around J. The process E-F is observed for $Ni_{78}Si_{10}B_{12}$, but not for $Pd_{80}Si_{20}$. The gradual decrease in C_p in the region B-C shows that there is an exothermic reaction which is attributed to structural relaxation. Then the temperature at B is considered to correspond to T_r, at which the structural relaxation starts. The discontinuous increase (C-D) in C_p observed after a dip is considered to be due to an endothermic reaction around the glass transition temperature. The temperature at C corresponds to the glass transition temperature. Chen and Turnbull[10-12] have measured the specific heat for Au-rich amorphous alloys of Au-Ge-Si system in the temperature range around the glass transition temperature using a differential scanning calorimeter. They also found a sharp increase in C_p at T_g depending on the heating rate, but not the dip related to the relaxation process below T_g.

Masumoto and coworkers[1-5] studied the crystallization process of $Ni_{78}Si_{10}B_{12}$ and $Pd_{80}Si_{20}$ metallic glasses in detail above the glass transition temperature using various kinds of measurements. According to their results, the amorphous phase transforms to a fully stable phase through a sequence of progressively more stable phases. In the case of amorphous $Pd_{80}Si_{20}$ alloy, a transformation sequence is identified as consisting of the following four successive stages: (1) the incipient stage of crystallization

(Am', amorphous); (2) the appearance of a number of small Pd crystallites with f.c.c structure within the amorphous matrix(MS-I, metastable I); (3) the formation of a complex ordered metastable phase (MS-II, metastable II) over the entire amorphous matrix with dispersed MS-I phase; (4) the final stage which produces the stable phases (ST, stable) consisting of Pd and Pd_3Si as shown in Fig.2. The temperature of the H-I region in the figure corresponds to the crystallization temperature Tx determined by Masumoto and co-workers. The inset in the figure is the isothermal electrical resistivity curve during heating and cooling of $Pd_{80}Si_{20}$ metallic glass measured by Masumoto and Maddin[5]. According to them, the abrupt decrease in the resistivity at about 350 °C signals the beginning of crystallization. The broad minimum occurring between 400 °C and 550 °C suggests the formation of metastable phases before equilibrium is achieved at 550 °C. As seen in the figure, the temperature at H and I-J-K in C_p-T curve correspond approximately to those at H' and I'-J'-K' in the ρ -T curve, respectively. The rapid decrease in C_p from J to K is considered to be due to a fully stable stage being reached.

Figures 3 (a)-(d) show the DSC curves for the $Pd_{80}Si_{20}$ metallic glass(sample 1), which were measured at various heating rate. As the crystallization temperature T_x is defined to correspond the temperature of initial stage of crystallization, T_x increases as the heating rate α (K·s^{-1}) increases as seen in the figures. It was found that T_x increases almost linearly with ln α . Kissinger's equation $d(\ln T_x^2/\alpha)/d(1/T_x) = E/R$ (E= activation energy: R= gas constant) is usually used to determine the energy of activation for the first order reaction from the results of differential thermal studies. Figure 4 shows a Kissinger's plot for the present results, from the slopes of which the energy of activation E is estimated to be 61 kcal·gramatom[-1].
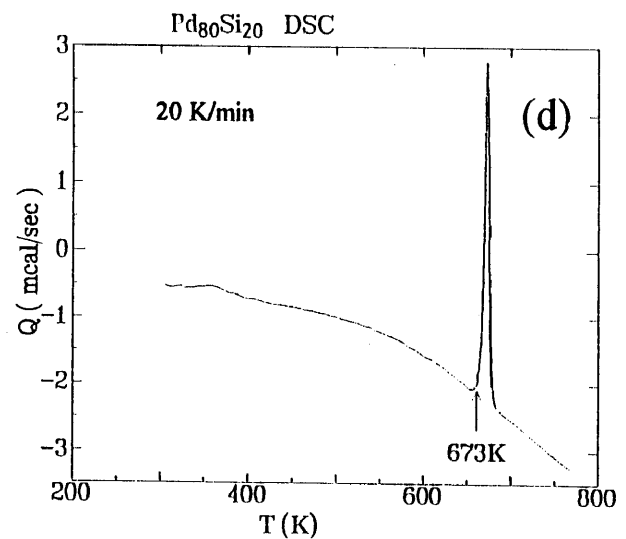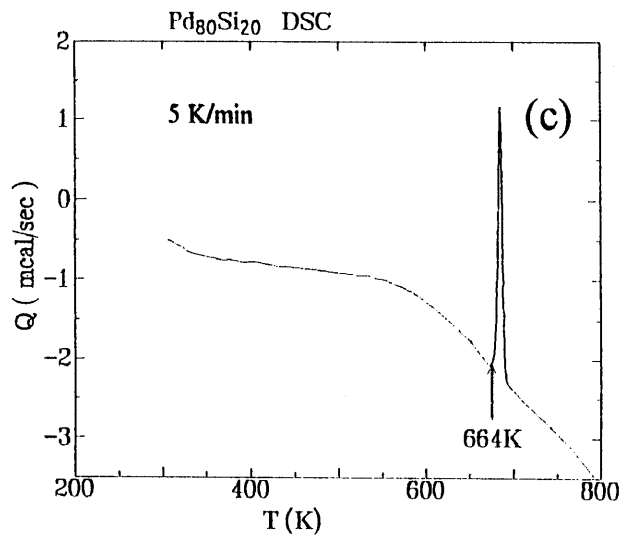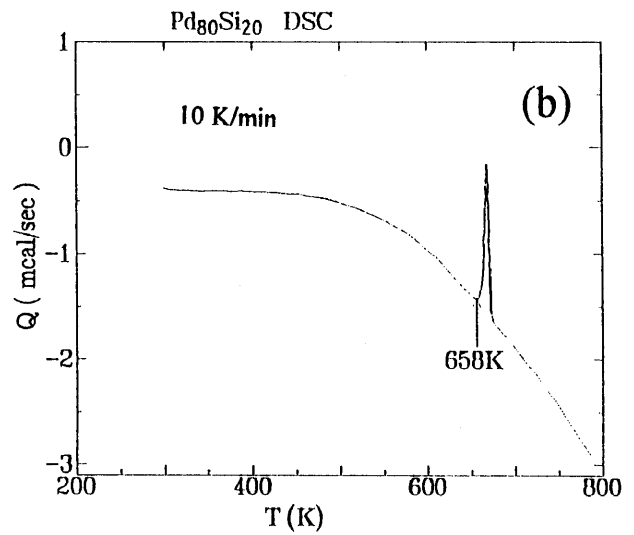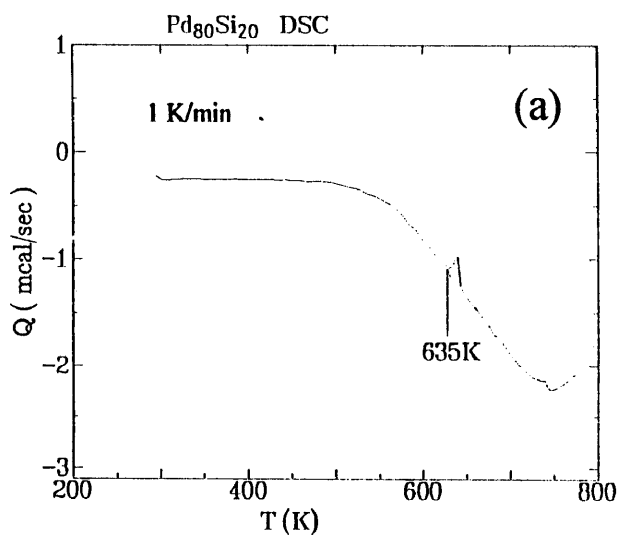

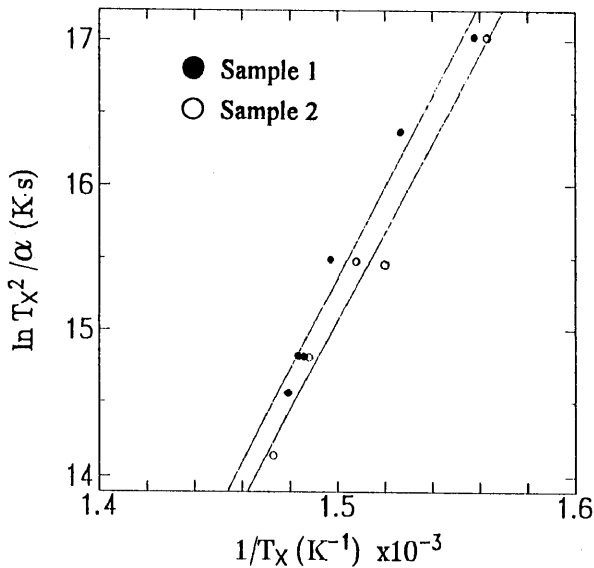Fig. 3. Differential scanning calorimetric (DSC) curves at various heating rates.

Fig. 4. Kissinger's plot for $Pd_{80}Si_{20}$ metallic glasses.
(● : sample 1 and ○ : sample 2).

3.2 $Zr_{60}Al_{15}Cu_{15}Ni_{7.5}Co_{2.5}$, $Zr_{65}Al_{7.5}Cu_{27.5}$ and $Zr_{67}Cu_{33}$

Figure 5 shows the DSC curve for the prepared $Zr_{60}Al_{15}Cu_{15}Ni_{7.5}Co_{2.5}$ metallic glass, which was measured at the heating rate of 5 K·min⁻¹. In the DSC curve are observed the anomalies by endothermic reaction and a peak by exothermic one, which are ascribed to the glass transition and crystallization, respectively. We defined here T_g and T_x as shown with arrows in the figure, which correspond to the temperature of initial stage of the glass transition and crystallization, respectively. And then T_m is the temperature of exothermic peak of the DSC curve. T_g, T_x and T_m were obtained to be 660 K, 720 K ands 748 K, respectively. T_g is in good agreement with the value given by Kimura et al.[2]. However, T_x and T_m are larger
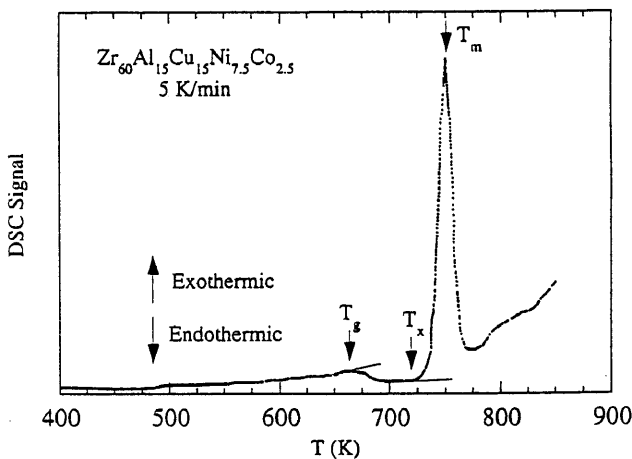

Fig. 5. Differential scanning calorimetric (DSC) curves of $Zr_{60}Al_{15}Cu_{15}Ni_{7.5}Co_{2.5}$ metallic glass.

than the values reported by Kimura et al.. It should be noted that the DSC curve of $Zr_{60}Al_{15}Cu_{15}Ni_{7.5}Co_{2.5}$ observed by Kimura et al.[2] was measured at the heating rate of 40 K·min⁻¹. The temperature range ΔT_x of the supercooled liquid region is estimated to be 60 K. Kimura et al.[2] have studied the heating rate dependence of T_g and T_x for $Zr_{60}Al_{15}Cu_{15}Ni_{7.5}Co_{2.5}$ metallic glass. According to their results, T_x is 718 K and 768 K for the heating rate of 4.8 and 40 K·min⁻¹, respectively. T_x increases with increase of the heating rate . On the other hand, T_g is not so dependent on the heating rate, but about 650 K for the heating rates through 4.8 and 40.2 K·min⁻¹. ΔT_x increases with increasing heating rate.
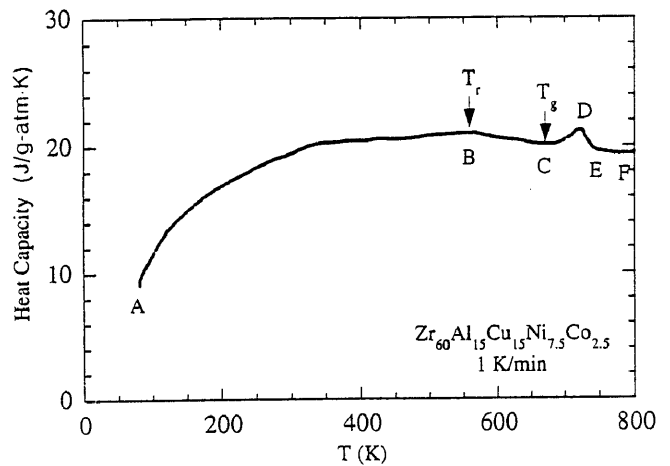

Fig. 6. Temperature dependence of the specific heat of $Zr_{60}Al_{15}Cu_{15}Ni_{7.5}Co_{2.5}$ metallic glass.

Figure 6 shows a specific heat C_p vs. temperature T curve for $Zr_{60}Al_{15}Cu_{15}Ni_{7.5}Co_{2.5}$ metallic glass. The specific heat was measured at the heating rate of 1 K·min⁻¹. As seen in the figure, the temperature dependence of the specific heat can be characterized as follows: (1) The specific heat increases at first with increasing temperature (A-B). (2) It decreases after reaching a broad maximum around $B(T_r)(B-C)$. (3) It increases monotonously at T_g (C-D). (4) It decreases sharply at temperatures from D to E. (5) Finally, it reaches a constant value. The gradual decrease in C_p in the region B-C shows that there is an exothermic reaction which is attributed to structural relaxation. Then the temperature at B is considered to correspond to T_r, at which the structural relaxation starts. T_r is found to be 559 K. Similar behaviors were observed in C_p-T curves of $Pd_{80}Si_{20}$ and $Ni_{78}Si_{10}B_{12}$ metallic glasses shown in Figures (1) and (2). The temperature of point C corresponds to T_g in the DSC curve in Fig.5. The experimental determination of T_g for Fig's. 5 and 6 is based on the extrapolation method, the extrapolation being achieved from the linear part of a high temperature supercooled liquid and from the linear part of a low temperature glass. The temperature at D (~724 K) corresponds to one of

exothermic peak of DSC curve.

Figure 7 shows the C_p vs. T curve for $Zr_{65}Al_{7.5}Cu_{27.5}$ metallic glass measured at the heating rate of 5 $K \cdot min^{-1}$. As seen in the figure, this temperature dependence of C_p is very similar to that of $Zr_{60}Al_{15}Cu_{15}Co_{2.5}Ni_{7.5}$ metallic glass in Fig.6.

Figure 8 shows the C_p vs. T curves of $Zr_{60}Al_{15}Cu_{15}Ni_{7.5}Co_{2.5}$ metallic glass measured by various heating rates. As shown in the figure, T_r and T_g do not depend on the heating rate. The temperature of the peak of C_p for each heating rate corresponds to T_m in DSC curve measured by the same heating rate. T_m and the height of the peak of C_p increase with increase of the heating rate. Therefore, T_x, which corresponds to the temperature of initial stage of crystallization, exists in the temperature region from T_g to T_m.

Figures 9(a)–(d) also show the C_p vs. T curves of $Zr_{67}Cu_{33}$ metallic glass measured by various heating rate. T_m and the height of the peak of C_p increase with increase of the heating rate as well as those of $Zr_{60}Al_{15}Cu_{15}Ni_{7.5}Co_{2.5}$ metallic glass.
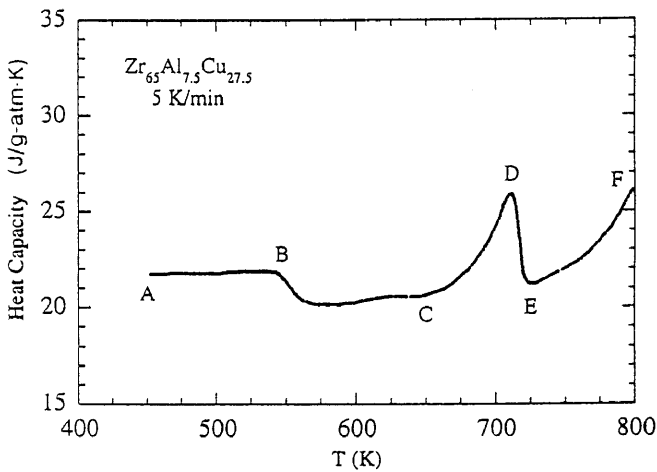

Fig. 7. Temperature dependence of the specific heat of $Zr_{65}Al_{7.5}Cu_{27.5}$ metallic glass.
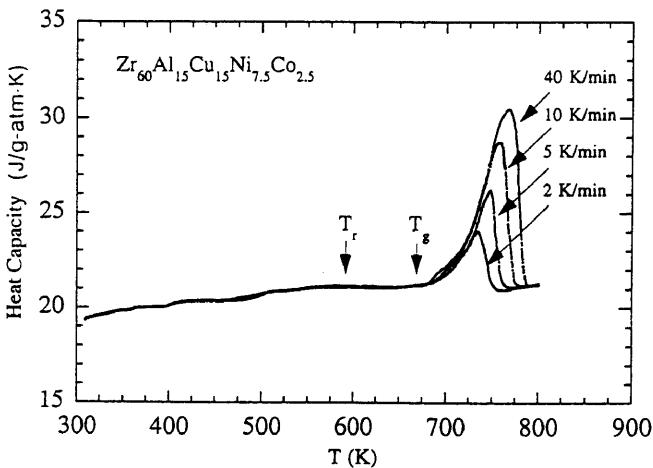

Fig. 8. Temperature dependence of the specific heat of $Zr_{60}Al_{15}Cu_{15}Ni_{7.5}Co_{2.5}$ metallic glass at various heating rates.
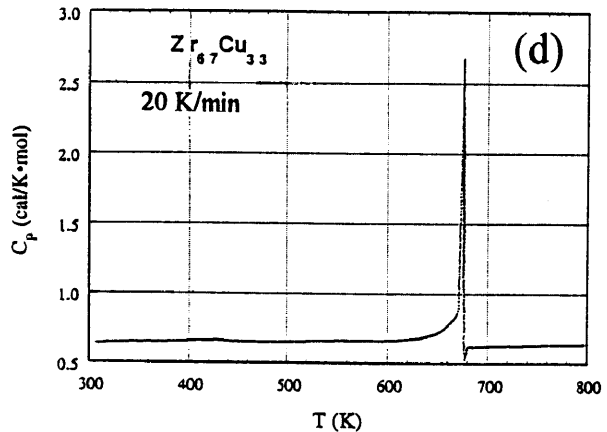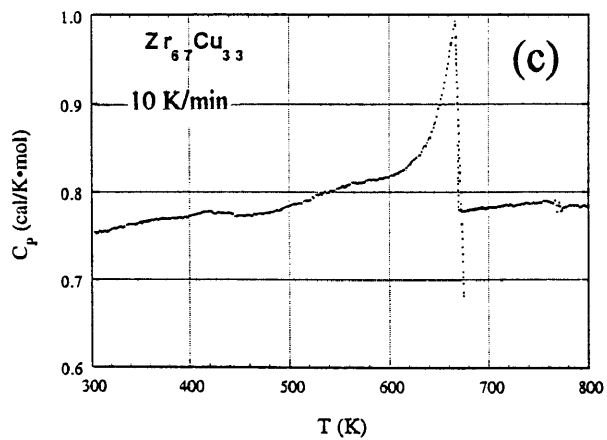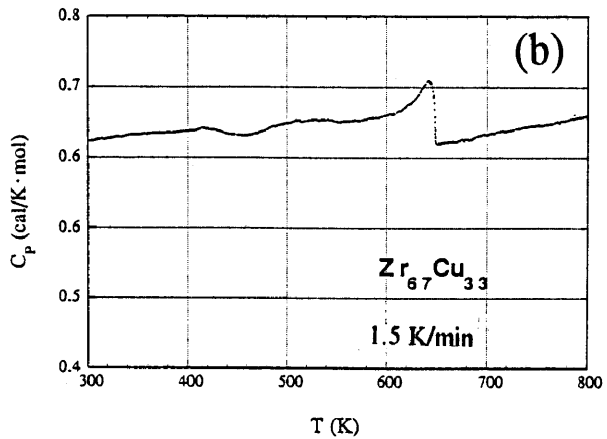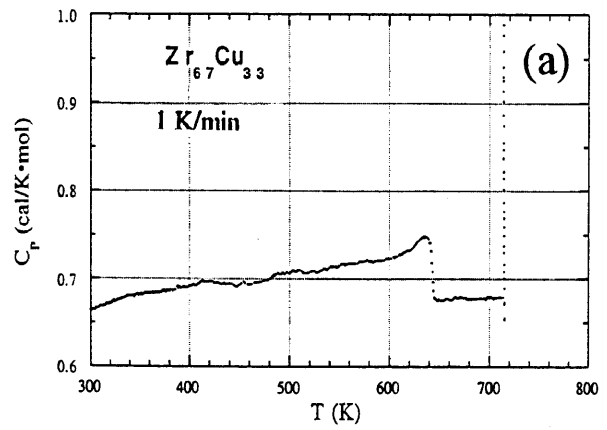

Fig. 9. Temperature dependence of the specific heat of $Zr_{67}Cu_{33}$ metallic glass at various heating rates.

As shown in Figure (1) and (2), C_p for $Ni_{78}Si_{10}B_{12}$ and $Pd_{80}Si_{20}$ metallic glasses increases at first with increasing temperature. Then it decreases after reaching a broad maximum around T_r. This temperature variation of C_p is very similar to that of $Zr_{60}Al_{15}Cu_{15}Ni_{7.5}Co_{2.5}$ metallic glass. On reaching to T_g, C_p increases discontinuously for $Pd_{80}Si_{20}$ and $Ni_{78}Si_{10}B_{12}$ metallic glasses, showing a maximum at T_g. On the other hand, C_p of $Zr_{60}Al_{15}Cu_{15}Co_{2.5}Ni_{7.5}$, $Zr_{65}Al_{7.5}Cu_{27.5}$ and $Zr_{67}Cu_{33}$ metallic glasses shows the monotonous change at T_g as shown in Figures 6, 7, 8 and 9.

For the characteristic features of the manifestation of the glass transition in C_p, there are two categories of materials: those showing a monotonous change and those showing a maximum at T_g[13].
In the former category are included "strong" network liquid, while some non-network substances belong to the later category. The higher is the degree of conformational freedom of a system, the wider the variety of behavior in the glass transition region and in the glassy state. The degree of structural freedom in the atomic configurations is expected to be highest in non-network system composed of spherical atoms. Examples of such systems are metals, metallic alloys and rare gases. In the case of $Pd_{80}Si_{20}$ and $Ni_{78}Si_{10}B_{12}$ metallic glasses, the atomic radius of the constituent elements Pd and Si, and Ni and Si are almost same. The amorphous structure has a more loose atomic configuration. Accordingly, these atoms become to be moved easily and abruptly at T_g, which results in the abrupt change of C_p due to the large change of conformational entropy.

As seen in Figures 6, 7, 8 and 9, the specific heat curves of $Zr_{60}Al_{15}Cu_{15}Co_{2.5}Ni_{7.5}$, $Zr_{65}Al_{7.5}Cu_{27.5}$ and $Zr_{67}Cu_{33}$ metallic glasses have the typical signature of a "strong" glass because of the lack of a peak at the glass transition. For Zr–Al–Cu metallic glasses, the atomic radius of the constituent elements are in order of Zr > Al > Cu. The intermediate atomic size of Al in the Zr–Al–Cu alloys was presumed to be appropriate to fill vacant sites in the disordered structure consisting of Zr and Cu with a large difference in atomic sizes, leading to an increase of the packing density in the amorphous solid and supercooled liquid. It was therefore presumed that the high stability originates partly from the increase of the packing fraction in the amorphous structure by the dissolution of Al. The increase of the packing density would result in a "strong" network. In other word, the constituent elements can not move easily even if the temperature increases through T_g. Therefore, the monotonous change of C_p at T_g observed in this study may be attributed to the strong network due to the increase of the packing density.

3. Conclusions

Thermal properties of the metallic glasses containing

Si and B ($Ni_{78}Si_{10}B_{12}$ and $Pd_{80}Si_{20}$) and the Zr–based metallic glasses ($Zr_{60}Al_{15}Cu_{15}Ni_{7.5}Co_{2.5}$, $Zr_{65}Al_{7.5}Cu_{27.5}$ and $Zr_{67}Cu_{33}$) are examined in the temperature range covering the glass transition temperature (T_g) and crystallization temperature (T_x) by a differential scanning calorimeter and a.c. specific heat calorimeter.

For Ni–Si–B and Pd–Si metallic glasses several exothermal and endothermal processes were observed correspondingly to the transformation sequence for complete crystallization. The structural relaxation process appears with a decrease in heat capacity. A discontinuous increase in the specific heat is observed at the glass transition temperature. For Zr–Cu based metallic glasses several exothermal and endothermal processes were also observed correspondingly to the transformation sequence for complete crystallization. The specific heat decreases in the temperature range of structural relaxation process below T_g and increases monotonously after making a minimum around T_g. With further increase of temperature C_p makes a peak and then decreases abruptly. The height of the peak of C_p increases with heating rate. It is concluded that the monotonous change of C_p at T_g for Zr–based metallic glasses may be attributed to the strong network due to the increase of the packing density by comparing with the temperature dependence of C_p for Ni–Si–B and Pd–Si metallic glasses.

1) T. Masumoto and R. Maddin, Acta Metall., 19(1971) 725.

2) R. Maddin and T. Masumoto, Mater. Sci. Eng., 9(1972) 153.

3) A. Inoue, T. Masumoto and H. M. Kimura, J. Jpn. Inst. Met. 42(1978) 303.

4) T. Masumoto, Y. Waseda, H. M. Kimura and A. Inoue, Sci. Rep. Res. Inst. Tohoku Univ., A26(1976) 21.

5) T. Masumoto, H. M. Kimura, A. Inoue and Y. Waseda, Mater. Sci. Eng., 23(1976) 141.

6) A. Inoue, T. Zhang and T. Masumoto, J. Non–Cryst. Solids, 156–158(1993) 473.

7) H. M. Kimura, M. Kishida, T. Kaneko, A. Inoue and T. Masumoto, Mater.Trans. JIM, 36(1995) 890.

8) T. Kanomata, H. Endo, M. Kuboki, H. M. Kimura, T. Kaneko and T. Masumoto, Mater. Sci. and Eng., A 179–180(1994) 351 .

9) T. Kanomata, Y. Sato, Y. Sugawara, H. M.

Kimura, T. Kaneko, A. Inoue and
T. Masumoto (to be published in J. Non-
Cryst. Solids)

10) H. S. Chen and D. Turnbull, J. Appl.
Phys. Lett., 10(1967) 284

11) H. S. Chen and D. Turnbull, J. Appl. Phys.,
38(1967) 3646

12) H. S. Chen and D.Turnbull, J. Chem.
Phys., 48(1971) 2560

13) F. Yonezawa, in Solid State Physics, vol.45
ed. by H. Ehrenreich and D. Turnbull,
(Academic Press, New York, 1991) P.186